Tryptophan to arginine substitution in puroindoline b alters binding to model eukaryotic membranes

Article

Published Version

It is advisable to refer to the publisher's version if you intend to cite from the work. See Guidance on citing.

To link to this article DOI: http://dx.doi.org/10.1021/acs.langmuir.6b03030

www.reading.ac.uk/centaur

LANGMUIR

# Tryptophan to Arginine Substitution in Puroindoline-b Alters Binding to Model Eukaryotic Membrane

Michael R. Sanders,[†] Luke A. Clifton,[‡] Richard A. Frazier,*,[†] and Rebecca J. Green*,[†]

[†]School of Pharmacy and Department of Food and Nutritional Sciences, University of Reading, PO Box 226, Whiteknights, Reading, Berkshire RG6 6AP, U.K.

[‡]ISIS Pulsed Neutron and Muon Source, Science and technology Facilities Council, Rutherford Appleton Laboratory, Harwell Oxford Campus, Didcot, Oxfordshire OX11 0QX, U.K.

S *Supporting Information*

ABSTRACT: We have studied how puroindoline-b (PINB) mutants bind to model eukaryotic membranes dependent on binary composition of anionic:zwitterionic phospholipids and the presence of cholesterol and sphingomyelin in the model membrane. We have found that the trends in lipid binding behavior are different for wild-type PINB compared to its naturally occurring PINB(Trp$_{44}$Arg) mutant form and have seen evidence of protein-induced domain formation within the lipid layer structure. Results show that selective binding of antimicrobial peptides to different membrane types is as a result of differences in lipid composition and the arrangement of lipids within the membrane surface. However, membrane-binding behavior is not easily predicted; it is determined by net charge, hydrophobicity, and the amphiphilicity of the protein/peptide lipid-binding domain.
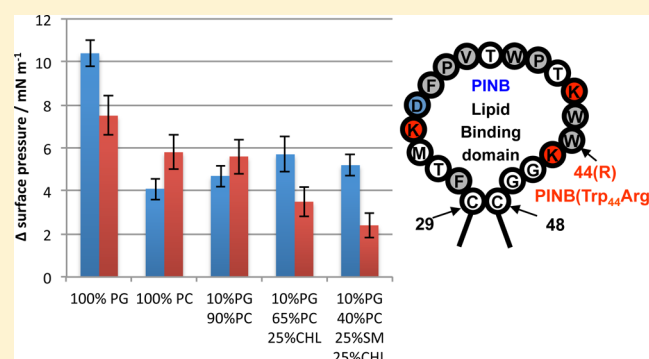
INTRODUCTION

Puroindolines (PINs) are cysteine-rich basic proteins with a mass of around 13 kDa isolated from wheat that contain a tryptophan-rich domain (TRD) presented by a disulfide bond.[1] Although the biological function of the PINs is unknown, it appears to involve the lipid-binding behavior of this family of proteins.[2] The PINs have been shown to have several hydrophobic regions that may be important for the protein−lipid interaction; it is thought that the TRD is likely to be key,[2] although there are point mutations that affect the behavior of PIN proteins that are not in the TRD.[3] There is not currently a high-resolution structure for any of the full-length isoforms, making it difficult to resolve the function of hydrophobic regions as a part of the full-length protein, but evidence for their function comes from work on homologous peptides of the TRD.[4−7] Much of this work also includes NMR structures of the TRD of PINB without the cysteine residues or Gly47,[6] originally resolved by cDNA sequencing.[8] Our previous work has focused on how mutations found in nature affect the lipid binding behavior of the PINs and how this relates to the role played in the grain hardness trait in wheat; however, the PINs have also been shown to have an active role in pathogenic defense shown both *in vivo* and *in vitro*.[9,10]

One of the main questions involved with the mechanism of antimicrobial proteins and peptides is, how are they able to differentiate between the membrane of host and pathogen? The phospholipid composition of eukaryotic cells is dominated by the zwitterionic phospholipid headgroup phosphatidylcholine (PC) with a small percentage of anionic headgroup component contributed by phosphatidyl-*rac*-glycerol (PG) or phosphatidylserine (PS) depending on the species and the cell type. For example, in human red blood cells, the PC headgroup makes up around 70% of total lipid content and 8% is PS, with a large proportion of the rest made up of cholesterol (CHL) and sphingomyelin (SM).[11] In comparison, in the cell membranes of eukaryotic nerve cells there is a larger proportion of anionic phospholipids in the membrane.[12] Consistent with the differences in lipid composition, PIN proteins interact with different eukaryotic cell types in different ways. *In vitro* studies carried out with PINA have shown that there was no hemophilic activity;[10] however, membrane structural changes occur in *in vitro* experiments using nerve cell axons.[12,13] This suggests that the lateral organization of the membrane, a combination of headgroup sizes, membrane charge, and fluidity,[14] has a major role in governing the interaction of antimicrobial peptides and host/pathogen selectivity.

The lipid metabolism of eukaryotic cells also integrates sterols into the cell membrane, and in-depth reviews have been written about the subject previously.[15,16] The presence of stigmasterol and cholesterol for plants and animals respectively modulate the fluidity and membrane thickness in eukaryotic cells. Sterols have been shown to localize within the acyl region

of the plasma membrane causing the formation of liquid-ordered (L$_O$) and liquid-disordered (L$_D$) phases in the membrane.[17,18] The L$_O$ phase shows a higher molecular density when compared with membranes composed of phospholipids only.[17] There are a number of examples that show membrane protein insertion[18] and anchoring[19] are affected by the phase of the membrane, and a number of membrane proteins have been shown to be affected specifically by the presence of cholesterol.[12] However, while L$_O$ phase effects on nonselective antimicrobial peptide (e.g., melittin) reorganization of cholesterol integrated membranes has been studied,[20,21] there is relatively little information available on how more selective defense proteins and peptides, such as the cathelicidin class of antimicrobial peptides (AMPs),[22,23] are able to differentiate between phospholipid head groups or how membrane fluidity takes any part within the protein−lipid interaction. *In vivo* the ability to phase separate the membrane into L$_O$ and L$_D$ regions allows the lateral formation of functional domains.[14] Furthermore, although not necessary for the formation of the L$_O$ phase, *in vivo* phase separated L$_O$/L$_D$ microdomains are rich in protein, CHL, and SM.[24,25]

In our previous work we have focused on the difference in binding behavior of the wild-type isoforms of the PINs and comparisons with naturally occurring mutants.[26−28] The differences between mutants characterized in these studies have been attributed to single amino acid substitutions in the TRD. Those studies focused on how only headgroup charge affected the selectivity of the different isoforms of the PINs and how mutations in the TRD affected that interaction, focusing on the role of the PINs with respect to wheat grain hardness. In subsequent work,[29] we characterized the lipid headgroup selectivity and interaction using more complex membrane models in the context of pathogenic defense, where we showed that the PINs are influenced by membrane fluidity when comparing binding to unsaturated and saturated lipids. More importantly, we showed that the lateral organization of a monolayer has significant effects on the protein−lipid interaction within PINB based upon comparisons to PINB-(Trp$_{44}$Arg), which has a Trp to Arg mutation within the TRD. A schematic of the differences in the TRD region of PINB and PINB(Trp$_{44}$Arg) is shown in Figure 1. By modeling different components of the bacterial lipid membrane, we showed that different characteristics of the lipids within the membrane dictate protein−lipid interaction but that the binding of PINB and PINB(Trp$_{44}$Arg) is affected differently by the lateral

organization of lipids within the membrane. It has been discussed elsewhere that key amino acid residues, like Trp and Arg within the TRD of the PINs, determine the mode of binding to a lipid membrane.[5−7]

In previous work, we have studied PIN binding to pure lipid layers[28] and to mixed lipid systems that are associated with the lipid composition of bacterial membranes.[29] Here, we extend our studies to model PIN binding to models based upon eukaryotic membranes. We use a monolayer membrane model in order to better control the phase and lipid composition in the context of the protein−lipid interaction. The aim of the work is to better understand the role played by the host lipid components of biological membranes in the context of antimicrobial protein binding. Surface pressure (which measures total amount of protein inserted at the interface), external reflection FTIR spectroscopy (measuring total amount of protein adsorbed at the interface), and Brewster angle microscopy (which looks at lateral organization of the monolayer) have all been used in order to directly compare the effects of interaction of the PINb and PINB(Trp$_{44}$Arg) with the mixed lipid monolayers composed of eukaryotic membrane lipids.

■ MATERIALS AND METHODS

Materials. Lipids were obtained as powders from Avanti Polar Lipids (Madison, WI) without further purification. Lipid powders were suspended in HPLC chloroform (Sigma-Aldrich) as stock solutions of 1 mg/mL. The multiple lipid solutions were prepared to give a total lipid concentration of 1 mg/mL. Buffers were made from a combination of monosodium phosphate and disodium phosphate (dihydrate) to make buffer strength of 20 mM with a pH or pD 7.0. UHQ water was used for all solutions used in surface pressure and BAM experiments, and D$_2$O was used as the solvent for FTIR experiments. UHQ water was obtained from an ELGA water purifier and 99.9% D$_2$O was obtained from Sigma-Aldrich. PINB and PINB(Trp$_{44}$Arg) were purified from Claire and Soissons wheat varieties, respectively (Table 1 shows the full genotype and

Table 1. Expression Genotypes of the Wheat Varieties Used To Purify PINB and PINB(Trp$_{44}$Arg)

wheat variety	genetic designation		molecular designation		
	Pina	Pinb	protein	mutation	phenotype
Claire	Pina-D1a	Pinb-D1a	PINB	wild type	soft
Soissons	Pina-D1a	Pinb-D1d	PINB(Trp$_{44}$Arg)	Trp44 to Arg44	hard

phenotypes of the wheat varieties), using Triton X-114 phase partitioning and chromatography techniques as described elsewhere.[26,30] SDS-PAGE (Figure S1) and non-native mass spectrometry (Figure S2) were used to determine the purity of both proteins, which indicate their separation from PINA, PINB2, and grain softness protein-1 (GSP-1).

Surface Pressure Measurements. Surface pressure measurements were carried out using the method described previously.[31] Briefly, a Langmuir Teflon trough (model 611, Nima technology Ltd., Coventry, UK) was used to prepare lipid monolayers that were compressed and held in the condensed phase at 22 mN/m. Following our previous methodology,[26,29,31] the protein was added to the subphase of the stabilized lipid layer to provide a final concentration of protein in the subphase of 0.48 μM PINB or PINB(Trp$_{44}$Arg). Changes in surface pressure were observed for 150 min after protein injection and plotted as surface pressure vs time. All systems were repeated in triplicate, and statistical analysis was carried out to evaluate
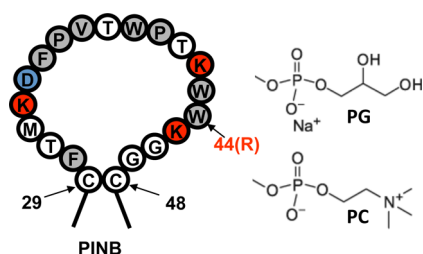

Figure 1. Primary structure of the tryptophan-rich domain of PINB,[8] which indicates the position of the Trp to Arg point mutation leading to PINB(Trp$_{44}$Arg) (charged amino acids in red (cationic) and blue (anionic) and hydrophobic amino acid (gray)). The headgroup structures of phospholipids used in this study are also provided: phosphatidyl-*rac*-glycerol (PG) and phosphatidylcholine (PC). We have depicted the TRD contained within a loop between Cys 29 and Cys 48 as postulated by Douliez et al.[1]

level of difference between observed changes in surface pressure using one-way ANOVA and Tukey HSD *posthoc* test.

Brewster Angle Microscopy. A Nanofilm EP3 imaging ellipsometer (Nanofilm Technology, Goettingen, Germany) mounted above a Langmuir trough (model 302a, Nima, Coventry, UK) was used to obtain BAM images. Surface pressure and film morphology could be monitored simultaneously using this setup. As described previously,[27] the imaging ellipsometer was equipped with a frequency-doubled Nd:YAG laser (532 nm, 20 mW), 10× magnification objective, polarizer, analyzer, and CCD camera and was situated on an antivibration table. Lipid monolayers and protein addition to the layers were prepared as described for surface pressure experiments. The surface pressure was monitored for 180 min after protein addition, and BAM images were captured at regular intervals after the protein addition to the subphase to monitor surface morphology.

External Reflection FTIR Spectroscopy. ER-FTIR spectra were recorded using a Thermo Nicolette Nexus instrument fitted with a monolayer/grazing angle accessory and a 10 mL trough.[31] In each experiment, 9.5 mL of 20 mM sodium phosphate buffer (pD 7.0) was placed in the trough, and a background single beam spectrum was recorded allowing time for the sample chamber purge to remove H_2O vapor and CO_2 from the atmosphere. After recording a background, lipid solution was spread on to the surface of the buffer and compressed to 22 mN/m in the condensed phase. Sample scans were taken after compression to ensure stability of the lipid film, monitored through the observation of the CH_2 symmetric and asymmetric stretching frequencies in the phospholipid tails shown in the regions 2854−2850 and 2924−2916 cm^{-1}, respectively. Protein solution was injected into the subphase in sequential experiments to make a final protein concentration respective to PINB or PINB($Trp_{44}Arg$) of 0.48 μM. Spectra were continuously collected from the moment of protein injection for 15 min followed by a single spectrum collection every 15 min to a total time of 120 min after protein injection. The interaction of the protein with the lipid monolayer was observed by monitoring the amide I region, 1700−1600 cm^{-1}.

To correct for any water vapor present, H_2O and HOD spectra were scaled and subtracted against protein adsorbed spectrum; the degree of subtraction was dependent on the adsorption time as well as the amount of H/D exchange. The HOD spectra used for scaling and subtraction purposes were collected during the purge of the sample area between single beam background collection and the addition of the lipid film. No further processing was performed to the data.

■ RESULTS

Lipid Layer Characterization. Figure 2 shows pressure−area isotherms of a binary DPPG:DPPC lipid monolayer and with addition of CHL and SM. BAM images are provided for the PG:PC:CHL lipid layer. Data for the pure lipid monolayers confirm those observed previously in the literature (Figure S3).[22,23] Mixed PG/PC isotherms show the characteristic liquid extended-liquid-condensed phase transitions observed for the pure lipid systems. The only difference observed is that the surface pressure at which the phase transition occurs varies between 5 and 7 mN/m, and this relates to the relative amount of DPPC and DPPG within the monolayer. The isotherm for the 10:90 PG:PC system is shown as an example in Figure 2. When CHL or CHL/SM is added to the binary lipid composition (Figure 2a), there is no indication of the phase transition observed previously. BAM images taken of the CHL/PC/PG mixed system (Figure 2b) show no sign of the uniform phospholipid domains and instead show regions of phase separation into L_O and L_D domains that coalesce into fully L_O as the surface pressure increases. These large circular fluid domains caused by the presence of CHL have been identified before and were proposed by Radhakrishnan and McConnell.[32] In this system saturated lipid molecules pack in a specific way forming a uniform monolayer in the L_O phase, where the lipid
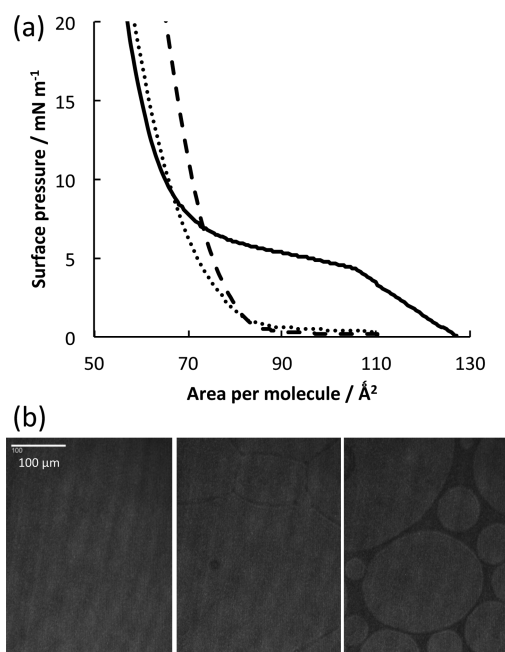

Figure 2. (a) Surface pressure vs area per molecule isotherms for systems containing 10:90 PG:PC (solid line), 10:65:25 PG:PC:CHL (dotted line), and 10:40:25:25 PG:PC:CHL:SM (dashed line). (b) BAM images taken during surface pressure monolayer compression for 65% DPPC 10% DPPG 25% CHL. Image on the right was taken at a surface area corresponding to the DPPC gaseous phase ($\sim$100 Å^2), the center image was taken during phase transition ($\sim$80 Å^2), and the image on the left is in the condensed phase ($\sim$65 Å^2).

acyl chains are packed against the planar structure of the sterol.[14]

PIN Interaction with Mixed Anionic:Zwitterionic Lipid Monolayers. Initial experiments focused on the interaction of PINB and PINB($Trp_{44}Arg$) with simple binary lipid systems of DPPG/DPPC. Figure 3 shows surface pressure measurements (as change in surface pressure) and data from FTIR spectra (as amide I peak area) for equilibrium adsorption of PINB and PINB($Trp_{44}Arg$) to these mixed DPPG/DPPC layers (Table S1). Data for the interactions to the pure lipids are provided as Supporting Information (Figures S4 and S5). We observe increasing penetration of both the wild type and the mutant into the lipid monolayer as the amount of PG in the layer increases, evidenced by changes in surface pressure. Changes in the total amount of protein within the interfacial region result from monitoring amide I peak area, and again the total amount is greater when the percentage of anionic lipid within the layer increases. However, the interaction does not simply correlate to the electrostatic interactions between PIN and the lipid head groups.

The amino acid substitution in PINB($Trp_{44}Arg$) leads to significantly less change in degree of penetration of the protein into the lipid layer (indicated by the surface pressure change) compared to PINB when the ratio headgroup composition of PG:PC is varied. Looking at the change in surface pressure for PINB($Trp_{44}Arg$), there was no significant difference in surface pressure change between binding to 100% PG surface and any PG:PC composition. Whereas, in the case of PINB, a significant reduction ($P < 0.05$) was measured for lipid layers with 20% and greater PC content with respect to 100% PG. In contrast, when monitoring the total amount of protein adsorbed, the total amount of PINB($Trp_{44}Arg$) adsorbed below the PG:PC
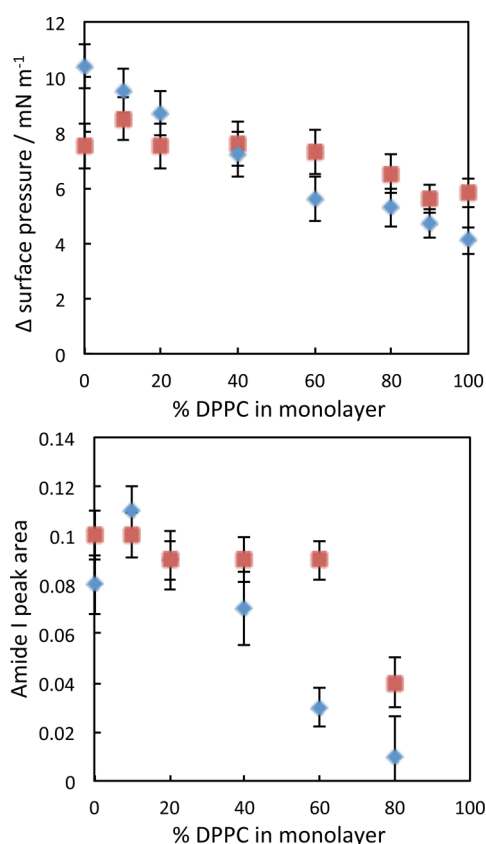
Figure 3. Changes in surface pressure (a) and amide I peak area (b) upon the addition of PINB (blue diamonds) and PINB(Trp$_{44}$Arg) (red squares) to binary phospholipid monolayers with increasing percentage of DPPC relative to the amount of DPPG within the monolayer.

Figure 4. Change in surface pressure ($\Delta\pi$) on addition of PINB (blue) and PINB(Trp$_{44}$Arg) (red) to mixed lipid monolayers. The asterisk denotes values that have statistically significant difference ($P < 0.05$) compared to 10% PG 90% PC sample.

lipid surface is either greater than or equal to that seen for PINB (determined from amide I peak area values). This suggests that PINB(Trp$_{44}$Arg) is able to adsorb to the surface of the lipid layer but not penetrate the lipid surface as effectively as PINB. As mentioned previously, these differences may be explained by increased net charge of PINB(Trp$_{44}$Arg) compared to PINB due to the additional basic residue (Arg) and reduced hydrophobicity of the PINB(Trp$_{44}$Arg) TRD resulting in less protein penetration into the acyl region of the lipid layer.[28,29]

Impact of the Lateral Lipid Organization on Protein–Lipid Interactions of PIN Proteins. Figure 4 and Table S2 show changes to monolayer penetration observed by surface pressure measurements of PINB and PINB(Trp$_{44}$Arg) when CHL and then SM are added to the total lipid content at ratios that match known eukaryotic membrane lipid composition,[8] with the amount of anionic lipid kept constant as complexity of the lipid composition studied is increased. CHL is an integral part of eukaryotic cell membranes and regulates membrane fluidity. Sterols are a necessary component to form the L$_O$ phase,[32] whereas SM is found in phase separated L$_O$/L$_D$ microdomains in vivo.[24]

When 25% cholesterol is added to the PG:PC lipid layer (as a percentage of the total lipid composition), it has an insignificant impact on PINB lipid layer penetration. When further adding SM to the lipid layer, the PC content was reduced to keep total zwitterionic component of the layer constant. This also has no impact on the magnitude of the
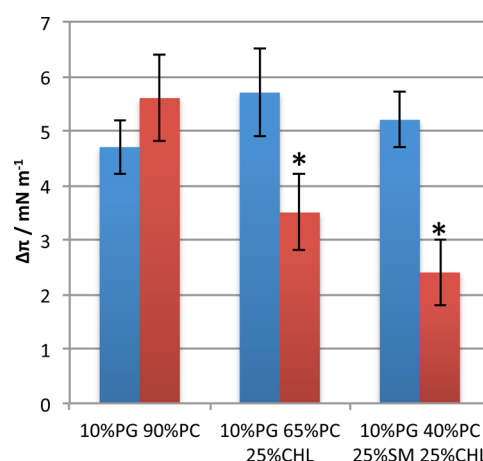
PINB–lipid interaction. These results suggest that the change in fluidity of the monolayer does not significantly impact on the interaction of PINB with the lipid surface. For PINB(Trp$_{44}$Arg) the findings are different: adding complexity (and thus potential for domain formation) and decreasing fluidity of the lipid layer reduces the ability of PINB(Trp$_{44}$Arg) to penetrate the lipid layer. Addition of CHL reduces the interaction, and addition of SM further reduces the interaction (a surface pressure change of 5.6 ± 0.8 mN/m for 10:90 PG:PC and reduced to 2.4 ± 0.6 mN/m for 10:40:25:25 PG:PC:SM:CHL). CHL will decrease the fluidity of the lipid layer, and studies have shown that in vivo SM associates in regions of L$_O$ phase so may exaggerate the effect of the added CHL.[24,25] These changes in lipid layer structure appear to reduce binding of the more polar and less hydrophobic binding domain of PINB(Trp$_{44}$Arg) while not affecting binding of PINB. Note that FTIR experiments are not shown since at this composition of DPPC/SM/CHL the small amount of signal seen for addition of protein made the experiments uninformative. We therefore focused on the surface pressure data, which is more sensitive to monolayer penetration rather than adsorption.

Figures 5 shows images taken using BAM microscopy in conjunction with surface pressure measurements for the adsorption of PINB and PINB(Trp$_{44}$Arg) to a 65% PC 10% PG 25% CHL monolayer in the L$_O$ phase. For PINB (Figure 5a), the BAM images reveal protein binding to the surface of the monolayer as regions of white (lighter image link to increased material at the surface). The adsorption of PINB causes the formation of material-dense regions that are localized showing evidence of ultradense regions within the L$_O$ monolayer. However, there is no evidence of phase separation between the L$_O$ and the L$_D$ phases. Our previous studies have shown BAM images for PIN binding to DPPG as uniform distribution of protein across the layer,[27,29] and we observe for PINB binding to DPPG a surface pressure change of 10.4 ± 0.6 mN/m.[29] Here PINB interaction with a mixed layer containing CHL shows localized binding of protein entirely consistent with a reduced surface pressure change of 5.7 ± 0.8 mN/m.

BAM images for PINB(Trp$_{44}$Arg) binding to 65% PC 10% PG 25% CHL lipid layer show no major change to the image, and this suggests less overall adsorption of material to this
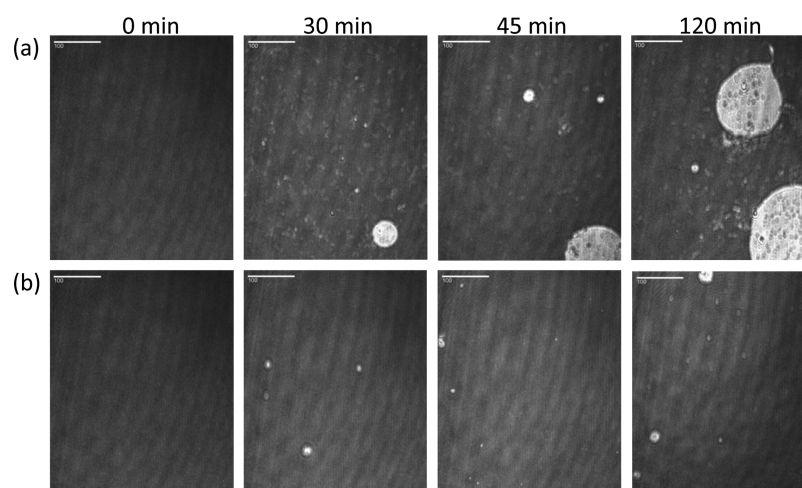
Figure 5. BAM images taken of the adsorption of (a) PINB and (b) PINB(Trp$_{44}$Arg) to a monolayer composed of 65:10:25 DPPC:DPPG:CHL Images taken at intervals of 0, 30, 45, and 120 min, and scale bars indicate 100 μm.

surface compared to that seen for PINB (Figure 5b), correlating well with the surface pressure change observed. Again there is no evidence of uniform protein adsorption, and the little amount of protein that has interacted with the monolayer has formed very small circular protein-rich domains, but again no evidence of phase separation. In contrast with the wild type, these dense protein domains do not grow bigger over time. This is further evidence that the presence of CHL within the monolayer limits the interaction of PINB(Trp$_{44}$Arg).

DISCUSSION

Our work has probed how lipid composition and lateral membrane organization within biological membranes can dictate host and pathogenic interactions of antimicrobial proteins and peptides with the cell membrane. This study focused on modeling protein−lipid interactions based upon the lipid composition of eukaryotic cell membranes[11] and complements our previous study that looked at membrane models based upon the lipid composition in bacterial cell membranes.[29] We have shown that the PIN−lipid interaction at binary anionic:zwitterionic lipid layers is not purely a result of electrostatic forces between lipid headgroup and the PIN lipid-binding TRD domain. There are selective differences between the wild type and the Trp to Arg mutant in terms of lipid binding behavior as the amount of anionic content within the monolayer decreases. The more hydrophobic wild type is significantly affected by the loss of electrostatic interaction, demonstrated as both less penetration and adsorption to the membrane, whereas the mutant shows no significant change to the amount of membrane penetration (Figure 3). As seen in Figure 6 (and Table S3), when the data are compared to our earlier work on bacterial membrane models[29] both wild-type PINB and PINB(Trp$_{44}$Arg) are able to differentiate between mixed lipid anionic:zwitterionic monolayers consisting of different zwitterionic lipids and thus the same net charge. Interestingly, the wild type is able to positively discriminate between bacterial membrane models containing a PE headgroup[29] and a host cell membrane model containing a PC headgroup (compare red (PG:PE) and blue (PE:PG) data in Figure 6a) showing greater protein penetration into the PG:PE (bacterial mimic) compared to the PG:PC lipid system.[28] The single Trp to Arg mutant is also able to discriminate between the host and the pathogen membrane mimics, but in a different
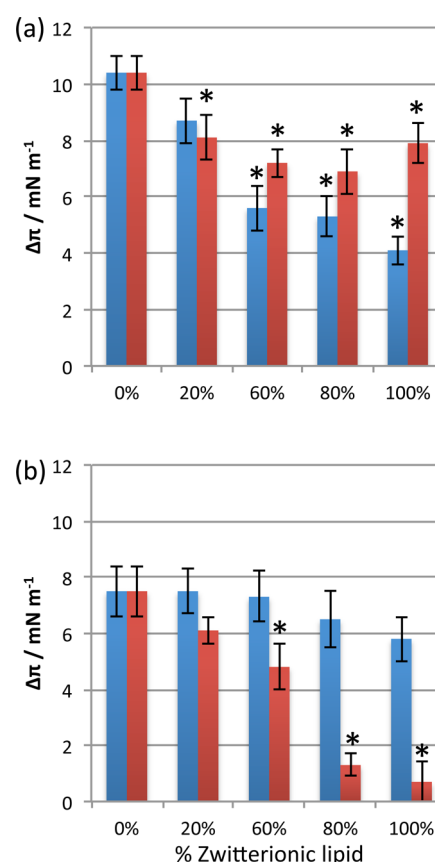

Figure 6. Change in surface pressure (Δπ) values on addition of PIN to binary mixtures of PG:zwitterionic phospholipids; PG:PC (blue) and PG:PE (red). Panel a shows wild-type PINB values, and panel b shows mutant PINB(Trp$_{44}$Arg) values. The asterisk denotes values that have statistically significant difference ($P < 0.05$) compared to 100% PG.

manner. In this case PIN(Trp$_{44}$Arg) does not interact with the PE headgroup at all, seen as no surface pressure change in Figure 6b, but is able to interact positively with the PC headgroup, resulting in a surface pressure change that is similar to that seen for binding to 100% PG. This effect has not been observed previously using bilayer models as the ability to

control headgroup composition is dependent upon the mixture being able to form a bilayer.[33] The impact of the lipid headgroup size and how this modifies the lateral organization of lipid molecules plays a part, as seen by the contrasting behavior of PIN binding to DPPC and DPPE containing lipid surfaces.

We have further demonstrated that as the complexity of the lipid layer composition is increased to incorporate cholesterol, the decreased fluidity of the layer limits penetration of PINB(Trp$_{44}$Arg). The interaction with the wild-type PINB is remarkably different, with the mixed PG:PC:CHL layer showing the formation and growth over time of superdense protein regions within the liquid ordered lipid surface. After initial penetration into the acyl region of the lipid,[27] we speculate that PINB strongly interacts with CHL forming circular protein-rich regions similar in shape to L$_O$ regions observed during monolayer compression.

There are many reports on the interaction of AMPs with membranes, with the most characterized examples, such as melittin, being unable to differentiate between different phospholipid head groups.[20,21] One of the notable families of AMPs that are able to differentiate between different membranes are the cathelicidins[23] that include indolicidin,[34] to which the TRD of the PINs shows a high homology.[7] Although the mechanism by which these peptides are able to select between different membranes is not fully resolved, the general consensus is that headgroup selectivity is primarily attributable to electrostatic interactions.[35] Our work has shown, in at least the case of full-length PIN proteins, that the lateral organization of complex membranes also significantly affects the selectivity of the protein for complex membranes of different lipid headgroup compositions and fluidity; showing specific selectivity between membranes composed of different head groups but the same overall charge.

To further gauge how selective the PINs could be to a host cell, we increased the complexity of the monolayer to integrate SM into the lateral organization. Although not necessary for the formation of the L$_O$ phase,[14] it has been found *in vivo* that SM localizes with CHL and proteins in transient highly dense microdomains.[24] Although we were not able to image these transient domains, the addition of SM further reduced binding of PINB(Trp$_{44}$Arg), but again did not influence PINB lipid penetration. This again demonstrates the impact of membrane fluidity on the interaction of the highly charged PINB-(Trp$_{44}$Arg). Our work suggests that the selective binding of antimicrobial peptides to different cell types results from differences in lipid composition, membrane fluidity, and the lateral organization of lipids within the membrane. However, membrane-binding behavior is not easily predicted; it is determined by net charge, hydrophobicity, and the amphiphilicity of the protein/peptide lipid-binding domain. A single point mutation of a 13 kDa protein results in completely altering the mechanism of interaction with the membrane.

These results clearly show differences in the lipid binding behavior of the mutant and wild-type protein that could significantly alter the antimicrobial behavior of PIN. Further analysis investigating lipid compositions found within fungal membranes will enable us to determine if these structural differences potentially impact more widely to other pathogenic properties. Our findings also suggest the hypothesis that mutations to PINB are evolutionary selections that may be linked to their role in plant defense, as has been previously suggested for the molecular evolution of homologous genes responsible for PINA protein expression.[36]

ASSOCIATED CONTENT

Ⓢ Supporting Information

The Supporting Information is available free of charge on the ACS Publications website at DOI: 10.1021/acs.langmuir.6b03030.

Protein purification data are provided in Figure S1 (PINB on 15% SDS-PAGE gel) and Figure S2 (deconvoluted mass spectrum from non-native mass spectroscopy); additional surface pressure and BAM data are provided in Figure S3 (surface pressure isotherms and BAM images for DPPG and DPPC) and Figure S4 (surface pressure vs time for PIN binding to DPPG and DPPC); Figure S5, FTIR spectroscopy results for PIN interaction with DPPG; data tables provided for Figure 3 (Table S1), Figure 4 (Table S2), and Figure 6 (Table S3) (PDF)

AUTHOR INFORMATION

Corresponding Authors

*E-mail r.a.frazier@reading.ac.uk (R.A.F.).
*E-mail rebecca.green@reading.ac.uk (R.J.G.).

ORCID Ⓘ

Rebecca J. Green: 0000-0001-6783-549X

Notes

The authors declare no competing financial interest.

ACKNOWLEDGMENTS

ABBREVIATIONS

DPPC, 1,2-dipalmitoyl-*sn*-glycero-3-phosphocholine; DPPG, 1,2-dipalmitoyl-*sn*-glycero-3-phospho-(1′-*rac*-glycerol); DPPE, 1,2-dipalmitoyl-*sn*-glycero-3-phosphoethanolamine; ER-FTIR, external reflection Fourier transform infrared; BAM, Brewster angle microscopy; PIN, puroindoline; UHQ, ultrahigh quality.

REFERENCES

(1) Douliez, J. P.; Michon, T.; Elmorjani, K.; Marion, D. Mini Review: Structure, Biological and Technological Functions of Lipid Transfer Proteins and Indolines, the Major Lipid Binding Proteins from Cereal Kernels. *J. Cereal Sci.* **2000**, *32*, 1−20.

(2) Marion, D.; Bakan, B.; Elmorjani, K. Plant Lipid Binding Proteins: Properties and Applications. *Biotechnol. Adv.* **2007**, *25*, 195−197.

(3) Bhave, M.; Morris, C. F. Molecular Genetics of Puroindolines and Related Genes: Allelic Diversity in Wheat and Other Grasses. *Plant Mol. Biol.* **2008**, *66*, 205−219.

(4) Alfred, R. L.; Palombo, E. A.; Panozzo, J. F.; Bhave, M. The Antimicrobial Domains of Wheat Puroindolines are Cell-Penetrating Peptides with Possible Intracellular Mechanisms of Action. *PLoS One* **2013**, *8* (10), e75488.

(5) Andrushchenko, V. V.; Vogel, H. J.; Prenner, E. J. Solvent-Dependent Structure of Two Tryptophan-Rich Antimicrobial Peptides and their Analogs Studied by FTIR and CD Spectroscopy. *Biochim. Biophys. Acta, Biomembr.* **2006**, *1758*, 1596−1608.

(6) Haney, E. F.; Petersen, A. P.; Lau, C. K.; Jing, W.; Storey, D. G.; Vogel, H. J. Mechanism of Action of Puroindoline Derived Tryptophan-Rich Antimicrobial Peptides. *Biochim. Biophys. Acta, Biomembr.* **2013**, *1828*, 1802−1813.

(7) Chan, D. I.; Prenner, E. J.; Vogel, H. J. Tryptophan- and Arginine-Rich Antimicrobial Peptides: Structures and Mechanisms of Action. *Biochim. Biophys. Acta, Biomembr.* **2006**, *1758*, 1184−1202.

(8) Gautier, M. F.; Aleman, M. E.; Guirao, A.; Marion, D.; Joudrier, P. Triticum-Aestivum Puroindolines, 2 Basic Cysteine-Rich Seed Proteins - CDNA Sequence-Analysis and Developmental Gene-Expression. *Plant Mol. Biol.* **1994**, *25*, 43−57.

(9) Alfred, R. L.; Palombo, E. A.; Panozzo, J. F.; Bariana, H.; Bhave, M. Stability of Puroindoline Peptides and Effects on Wheat Rust. *World J. Microbiol. Biotechnol.* **2013**, *29*, 1409−1419.

(10) Capparelli, R.; Palumbo, D.; Iannaccone, M.; Ventimiglia, I.; Di Salle, E.; Capuano, F.; Salvatore, P.; Amoroso, M. G. Cloning and Expression of Two Plant Proteins: Similar Antimicrobial Activity of Native and Recombinant Form. *Biotechnol. Lett.* **2006**, *28*, 943−949.

(11) de Oliveira, S.; Saldanha, C. An Overview about Erythrocyte Membrane. *Clin. Hemorheol. Microcirc.* **2010**, *44*, 63−74.

(12) Llanos, P.; Henriquez, M.; Minic, J.; Elmorjani, K.; Marion, D.; Riquelme, G.; Molgo, J.; Benoit, E. Neuronal and Muscular Alterations Caused by Two Wheat Endosperm Proteins, Puroindoline-a and Alpha1-Purothionin, are due to Ion Pore Formation. *Eur. Biophys. J.* **2004**, *33*, 283−284.

(13) Llanos, P.; Henriquez, M.; Minic, J.; Elmorjani, K.; Marion, D.; Riquelme, G.; Molgo, J.; Benoit, E. Puroindoline-a and Alpha 1-Purothionin Form Ion Channels in Giant Liposomes but Exert Different Toxic Actions on Murine Cells. *FEBS J.* **2006**, *273*, 1710−1722.

(14) Nyholm, T. K. M. Lipid-Protein Interplay and Lateral Organization in Biomembranes. *Chem. Phys. Lipids* **2015**, *189*, 48−55.

(15) Grouleff, J.; Irudayam, S. J.; Skeby, K. K.; Schiott, B. The Influence of Cholesterol on Membrane Protein Structure, Function, and Dynamics Studied by Molecular Dynamics Simulations. *Biochim. Biophys. Acta, Biomembr.* **2015**, *1848*, 1783−1795.

(16) Wustner, D.; Solanko, K. How Cholesterol Interacts with Proteins and Lipids During its Intracellular Transport. *Biochim. Biophys. Acta, Biomembr.* **2015**, *1848*, 1908−1926.

(17) Khelashvili, G.; Harries, D. How Cholesterol Tilt Modulates the Mechanical Properties of Saturated and Unsaturated Lipid Membranes. *J. Phys. Chem. B* **2013**, *117*, 2411−2421.

(18) Song, Y.; Kenworthy, A. K.; Sanders, C. R. Cholesterol as a Co-Solvent and a Ligand for Membrane Proteins. *Protein Sci.* **2014**, *23*, 1−22.

(19) Brown, D. A.; Rose, J. K. Sorting of GPI-Anchored Proteins to Glycolipid-Enriched Membrane Subdomains During Transport to the Apical Cell Surface. *Cell* **1992**, *68*, 533−544.

(20) Qian, S.; Heller, W. T. Melittin-Induced Cholesterol Reorganization in Lipid Bilayer Membranes. *Biochim. Biophys. Acta, Biomembr.* **2015**, *1848*, 2253−2260.

(21) Qian, S.; Rai, D.; Heller, W. T. Alamethicin Disrupts the Cholesterol Distribution in Dimyristoyl Phosphatidylcholine−Cholesterol Lipid Bilayers. *J. Phys. Chem. B* **2014**, *118*, 11200−11208.

(22) da Silva, F. P.; Machado, M. C. C. Antimicrobial Peptides: Clinical Relevance and Therapeutic Implications. *Peptides* **2012**, *36*, 308−314.

(23) Wong, J. H.; Ye, X. J.; Ng, T. B. Cathelicidins: Peptides with Antimicrobial, Immunomodulatory, Anti-Inflammatory, Angiogenic, Anticancer and Procancer Activities. *Curr. Protein Pept. Sci.* **2013**, *14*, 504−514.

(24) Quinn, P. J. Structure of Sphingomyelin Bilayers and Complexes with Cholesterol Forming Membrane Rafts. *Langmuir* **2013**, *29*, 9447−9456.

(25) Radhakrishnan, A.; Anderson, T. G.; McConnell, H. M. Condensed Complexes, Rafts, and the Chemical Activity of Cholesterol in Membranes. *Proc. Natl. Acad. Sci. U. S. A.* **2000**, *97*, 12422−12427.

(26) Clifton, L. A.; Green, R. J.; Frazier, R. A. Puroindoline-b Mutations Control the Lipid Binding Interactions in Mixed Puroindoline-a: Puroindoline-b Systems. *Biochemistry* **2007**, *46*, 13929−13937.

(27) Clifton, L. A.; Green, R. J.; Hughes, A. V.; Frazier, R. A. Interfacial Structure of Wild-Type and Mutant Forms of Puroindoline-b Bound to DPPG Monolayers. *J. Phys. Chem. B* **2008**, *112*, 15907−15913.

(28) Clifton, L. A.; Lad, M. D.; Green, R. J.; Frazier, R. A. Single amino acid substitutions in puroindoline-b mutants influence lipid binding properties. *Biochemistry* **2007**, *46*, 2260−2266.

(29) Sanders, M. R.; Clifton, L. A.; Frazier, R. A.; Green, R. J. Role of Lipid Composition on the Interaction between a Tryptophan-Rich Protein and Model Bacterial Membranes. *Langmuir* **2016**, *32*, 2050−2057.

(30) Day, L.; Bhandari, D. G.; Greenwell, P.; Leonard, S. A.; Schofield, J. D. Characterization of Wheat Puroindoline Proteins. *FEBS J.* **2006**, *273*, 5358−5373.

(31) Lad, M. D.; Birembaut, F.; Clifton, L. A.; Frazier, R. A.; Webster, J. R. P.; Green, R. J. Antimicrobial Peptide-Lipid Binding Interactions and Binding Selectivity. *Biophys. J.* **2007**, *92*, 3575−3586.

(32) Radhakrishnan, A.; McConnell, H. M. Cholesterol-Phospholipid Complexes in Membranes. *Biophys. J.* **1999**, *76*, A431.

(33) Jelinek, R.; Kolusheva, S. Membrane Interactions of Host-Defense Peptides Studied in Model Systems. *Curr. Protein Pept. Sci.* **2005**, *6*, 103−114.

(34) Kim, S.-M.; Kim, J.-M.; Joshi, B. P.; Cho, H.; Lee, K.-H. Indolicidin-Derived Antimicrobial Peptide Analogs with Greater Bacterial Selectivity and Requirements for Antibacterial and Hemolytic Activities. *Biochim. Biophys. Acta, Proteins Proteomics* **2009**, *1794*, 185−192.

(35) Brender, J.; McHenry, A.; Ramamoorthy, A. Does Cholesterol Play a Role in the Bacterial Selectivity of Antimicrobial Peptides? *Front. Immunol.* **2012**, DOI: 10.3389/fimmu.2012.00195.

(36) Massa, A. N.; Morris, C. F. Molecular Evolution of the Puroindoline-a, Puroindoline-b, and Grain Softness Protein-1 Genes in the Tribe Triticeae. *J. Mol. Evol.* **2006**, *63*, 526−536.